



Swansea University
Prifysgol Abertawe



Cronfa - Swansea University Open Access Repository

This is an author produced version of a paper published in:
Optics Express

Cronfa URL for this paper:
<http://cronfa.swan.ac.uk/Record/cronfa22150>

Paper:

O'Keeffe, K., Lloyd, D. & Hooker, S. (2014). Quasi-phase-matched high-order harmonic generation using tunable pulse trains. *Optics Express*, 22(7), 7722-7732.
<http://dx.doi.org/10.1364/OE.22.007722>

This item is brought to you by Swansea University. Any person downloading material is agreeing to abide by the terms of the repository licence. Copies of full text items may be used or reproduced in any format or medium, without prior permission for personal research or study, educational or non-commercial purposes only. The copyright for any work remains with the original author unless otherwise specified. The full-text must not be sold in any format or medium without the formal permission of the copyright holder.

Permission for multiple reproductions should be obtained from the original author.

Authors are personally responsible for adhering to copyright and publisher restrictions when uploading content to the repository.

<http://www.swansea.ac.uk/library/researchsupport/ris-support/>

Quasi-phase-matched high-order harmonic generation using tunable pulse trains

Kevin O’Keeffe,* David T. Lloyd and Simon M. Hooker

Department of Physics, Clarendon Laboratory, Oxford University, Parks Road, Oxford OX1 3PU, UK

[*k.okeeffe1@physics.ox.ac.uk](mailto:k.okeeffe1@physics.ox.ac.uk)

Abstract: A simple technique for generating trains of ultrafast pulses is demonstrated in which the linear separation between pulses can be varied continuously over a wide range. These pulse trains are used to achieve tunable quasi-phase-matching of high harmonic generation over a range of harmonic orders up to the harmonic cut-off, resulting in enhancements of the harmonic intensity in excess of an order of magnitude. The peak enhancement of the harmonics is clearly shown to depend on the separation between pulses, as well as the number of pulses in the train, representing an easily tunable source of quasi-phase-matched high harmonic generation.

© 2014 Optical Society of America

OCIS codes: (190.4160) Multiharmonic generation; (320.5550) Pulses; (340.7480) X-rays, soft x-rays, extreme ultraviolet (EUV).

References and links

1. T. Popmintchev, M.C. Chen, D. Popmintchev, P. Arpin, S. Brown, S. Ališauskas, G. Andriukaitis, T. Balčiunas, O.D. Mücke, A. Pugzlys, A. Baltuška, B. Shim, S.E. Schrauth, A. Gaeta, C. Hernández-García, L. Plaja, A. Becker, A. Jaron-Becker, M.M. Murnane, and H.C. Kapteyn, “Bright Coherent Ultrahigh Harmonics in the keV X-ray Regime from Mid-Infrared Femtosecond Lasers,” *Science* **336**, 1287–1291 (2012).
2. J.C. Petersen, S. Kaiser, N. Dean, A. Simoncig, H.Y. Liu, A.L. Cavalieri, C. Cacho, I.C.E. Turcu, E. Springate, F. Frassetto, L. Poletto, S.S. Dhesi, H. Berger, and A. Cavalleri, “Clocking the Melting Transition of Charge and Lattice Order in $1T\text{-TaS}_2$ with Ultrafast Extreme-Ultraviolet Angle-Resolved Photoemission Spectroscopy,” *Phys. Rev. Lett.* **107**, 177402 (2011).
3. M. D. Seaberg, D. E. Adams, E. L. Townsend, D. A. Raymondson, W. F. Schlotter, Y. Liu, C. S. Menoni, L. Rong, C.-C. Chen, J. Miao, H. C. Kapteyn, and M. M. Murnane, “Ultrahigh 22 nm resolution coherent diffractive imaging using a desktop 13 nm high harmonic source,” *Opt. Express* **19**, 22470–22479 (2011).
4. M. Hentschel, R. Kienberger, Ch. Spielmann, G. A. Reider, N. Milosevic, T. Brabec, P. Corkum, U. Heinzmann, M. Drescher, and F. Krausz, “Attosecond metrology” *Nature (London)* **414**, 509–513 (2001).
5. A. Rundquist, C. G. Durfee III, Z. Chang, C. Herne, S. Backus, M. M. Murnane, and H. C. Kapteyn, “Phase-Matched Generation of Coherent Soft X-rays,” *Science* **280** 1412–1415 (1998)
6. E. A. Gibson, A. Paul, N. Wagner, R. Tobey, D. Gaudiosi, S. Backus, I. P. Christov, A. Aquila, E. M. Gullikson, D. T. Attwood, M. M. Murnane, and H. C. Kapteyn, “Coherent soft x-ray generation in the water window with quasi-phase matching,” *Science* **302**, 9598 (2003).
7. J. Seres, V. S. Yakovlev, E. Seres, C. Strelti, P. Wobrauschek, C. Spielmann, and F. Krausz, “Coherent superposition of laser-driven soft-x-ray harmonics from successive sources,” *Nat. Phys.* **3**, 878883 (2007).
8. M. Zepf, B. Dromey, M. Landreman, P. Foster, and S. M. Hooker, “Bright Quasi-Phase-Matched Soft-X-Ray Harmonic Radiation from Argon Ions,” **99**, 143901 (2007).
9. X. Zhang, A. L. Lytle, T. Popmintchev, X. Zhou, H. C. Kapteyn, M.M. Murnane, and O. Cohen, “Quasiphase-matching and quantum-path control of high-harmonic generation using counterpropagating light,” *Nat. Phys.* **3**, 270–275 (2007).
10. A. L. Lytle, X. Zhang, R. L. Sandberg, O. Cohen, H. C. Kapteyn, and M. M. Murnane, “Quasi-phase matching and characterization of high-order harmonic generation in hollow waveguides using counterpropagating light,” *Opt. Express* **16**, 65446566 (2008).

11. K. O’Keeffe and T. Robinson and S. M. Hooker “Quasi-phase-matching high harmonic generation using trains of pulses produced using an array of birefringent plates,” *Opt. Express* **20**, 6236–6247 (2012).
 12. A. Bahabad, M. Murnane, and H.C. Kapteyn, “Quasi-phase-matching of momentum and energy in nonlinear optical processes,” *Nat. Photonics* **4**, 570–575 (2010).
 13. R. Yano, and H. Gotoh, “Tunable terahertz electromagnetic wave generation using birefringent crystal and grating pair” *Jpn. J. Appl. Phys.* **44**, 8470-8473 (2005).
 14. T. Robinson, K. O’Keeffe, M. Landreman, S. M. Hooker, M. Zepf, and B. Dromey, “Simple technique for generating trains of ultrashort pulses” *Opt. Lett.* **32**, 2203-2205 (2007).
 15. T. Robinson, K. O’Keeffe, M. Zepf, B. Dromey, and S. M. Hooker, “Generation and control of ultrafast pulse trains for quasi-phase-matching high-harmonic generation” *J. Opt. Soc. Am. B* **27**, 763-772 (2010)
 16. M. Landreman, K. O’Keeffe, T. Robinson, M. Zepf, B. Dromey, and S. M. Hooker, “Comparison of parallel and perpendicular polarized counterpropagating light for suppressing high harmonic generation” *J. Opt. Soc. Am. B* **24**, 2421-2427 (2007).
 17. The Center for X-Ray Optics website: [www.cxro.lbl.gov].
 18. K. O’Keeffe, T. Robinson, S. M. Hooker, “Generation and control of chirped, ultrafast pulse trains” *J. Opt.* **12**, 015201 (2010).
-

1. Introduction

High harmonic generation (HHG) offers a straightforward approach for generating ultrafast pulses of coherent radiation with photon energies which can exceed 1keV [1]. The high degree of temporal and spatial coherence afforded by HHG makes it an attractive source for a host of applications including studies of ultrafast processes in condensed-matter systems [2], high-resolution imaging [3], and attosecond metrology [4]. However, the adoption of HHG in many applications is limited by poor conversion efficiency, resulting in low mean photon flux and low peak brightness. The low conversion efficiency of HHG is largely due to a phase mismatch between the driving laser field and the harmonics created at different points in the generating medium. This phase mismatch is the result of dispersion in the partially ionized medium in which harmonics are generated, and causes the intensity of each generated harmonic to oscillate with propagating distance between zero and some maximum value with an oscillation period of $2L_c$, where the coherence length $L_c = \pi/\Delta k_q$, and Δk_q is the wavevector mismatch given by $\Delta k_q = qk_0 - k_q$, where k_0 and k_q are the wave vectors of the fundamental and q^{th} harmonic, respectively. Therefore, in the presence of a phase mismatch the maximum harmonic intensity which can be achieved is that which can be generated over a single coherence length.

Under certain conditions it is possible to achieve true phase-matching ($\Delta k_q = 0$). For example, in the case of harmonics generated in a gas-filled hollow-core waveguide phase-matching can be achieved by balancing the waveguide and plasma dispersion with that of the neutral atoms [5]. This technique has been shown to dramatically increase the flux of harmonic sources. However, phase-matching of this type will only work up to a certain level of ionization above which it is no longer possible to balance dispersion. Since higher order harmonics are generated at higher laser intensities, this means that phase-matching can only be achieved up to a certain harmonic order.

Quasi-phase-matching (QPM) is an alternative technique for overcoming phase mismatch, in which harmonic generation is suppressed in regions where the locally generated harmonic radiation is out-of-phase with the harmonic beam. Suppressing multiple out-of-phase regions, or zones, allows the radiation from the remaining in-phase zones to combine coherently such that the output harmonic intensity can, in principle, be increased by a factor \mathcal{N}^2 above that for a single coherence length, where \mathcal{N} is the number of contributing zones. A significant advantage of QPM is that it can be achieved for all harmonics up to the harmonic cut-off.

QPM has previously been demonstrated using a variety of different methods. For example, QPM has been achieved through the use of hollow-core waveguides with modulated inner-diameters [6], by using spatially separated gas cells [7], or by utilizing mode beating in a capillary waveguide [8]. QPM can also be achieved using a train of counter-propagating laser

pulses [9, 10, 11]. For pulse train QPM (PTQPM) harmonic generation is suppressed in those regions in which the driving laser pulse overlaps with a counter-propagating pulse, with suppression being caused by a rapid variation in the phase of the harmonics as the driving pulse and counter-propagating pulses pass through each other, effectively scrambling harmonic generation in this region. A counter-propagating pulse train consisting of N pulses can suppress HHG in N separate regions, leaving $N + 1$ unsuppressed regions. Since the harmonic intensity of a quasi-phase-matched source scales with the square of the number of in-phase zones the harmonic intensity for PTQPM should scale as $\mathcal{N}^2 = (N + 1)^2$, so long as the pulses are suitably matched to L_c . In PTQPM the pulse train forms a modulation moving at a velocity of approximately $-c$ with respect to the driving pulse. It has been shown that spatiotemporal QPM leads to a shift in the frequency of the generated harmonics such that the q th harmonic has a frequency of $\Delta\omega_q = q\omega_0 - \Delta\omega$, where ω_0 is the frequency of the driving laser [12]. As a consequence the wave vector mismatch becomes $\Delta k_q = \Delta\omega n(\omega_q)/c + \Delta k'_q$, where $\Delta k'_q$ is the wave vector mismatch in the absence of a pulse train. For the case of a pulse train with period $\Lambda = w + d = 2w$, where w and d are the pulse width and separation, respectively, the correct matching condition to achieve QPM can be written as $d = 2mL_c$, where $m = 1, 2, 3, \dots$ is the order of the QPM process and L_c is the coherence length measured in the absence of the pulse train.

In previous experiments on PTQPM the required pulse trains were generated either by inserting glass plates inside a grating stretcher in order to generate different delays for different frequencies of a stretched pulse [9, 10], or by using a sequence of birefringent plates in which the thickness of each successive plate was doubled, producing a train of pulses with uniform pulse separation [11]. In both cases the width and separation of the pulses within the train is fixed by the choice of optical plates, determining the values of L_c which can be efficiently matched. In order to fully exploit the benefits of PTQPM simple techniques for generating versatile pulse trains are required, which allow the frequency of the QPM output to be tuned.

In this paper a simple technique for generating tunable pulse trains is shown to allow continuously-tunable QPM over a wide range of harmonic orders.

2. Generation of tunable pulse trains

A train of femtosecond-duration pulses may be generated by passing a single chirped pulse through a birefringent plate, as first described by Yano et al. [13], and subsequently by Robinson et al. [14]. In that technique a linearly-polarized chirped laser pulse is passed through a multiple-order waveplate orientated with its fast axis at 45° to the plane of polarization of the laser pulse. A linear polarizer is then placed after the waveplate such that its transmission axis is parallel to the original plane of polarization of the laser pulse. In order for light to be transmitted through the combination of polarizer and waveplate a phase-shift of $2n\pi$ (n an integer) must be introduced between the field components polarized parallel and perpendicular to the fast axis of the waveplate. This condition will only be met for certain frequencies and, since the pulse is chirped, the radiation transmitted by the polarizer will be modulated to form a train of pulses. For a linearly chirped laser pulse the spacing between pulses d will be approximately uniform across the train and given by

$$d = \frac{\pi c}{bl} \frac{1}{\beta'_{oe} - \beta'_{oo}} \quad (1)$$

where c is the speed of light, l is the thickness of the waveplate, b is the frequency chirp parameter (such that the instantaneous frequency is $\omega_0 + 2bt$), and $1/\beta'_{oe}$ and $1/\beta'_{oo}$ are the group velocities of the o and e rays, respectively [15]. For a given waveplate material, d is therefore determined by the thickness of the waveplate and the linear chirp of the stretched pulse.

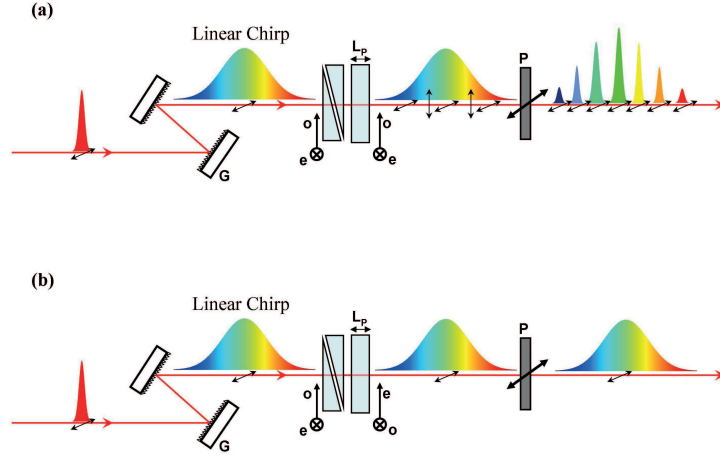


Fig. 1. Schematic of technique for generating tunable pulse trains. G: grating stretcher P: polarizer (a) Waveplate axes in same orientation as axes of wedge-pair so that $l' = \Delta L + L_p$. (b) Waveplate axes at 90° to axes of wedge-pair so that $l' = |\Delta L - L_p|$. Fig. (b) illustrates the case of $\Delta L = L_p$, such that $l' = 0$.

In order to match to arbitrary coherence lengths it would be desirable to be able to continuously tune the pulse separation d . From Eq. (1) it is clear that d can be varied by changing the thickness of the waveplate l . In the experiments described here l could be varied continuously over a wide range by using a multiple-order waveplate in combination with a pair of birefringent wedges, as illustrated in Fig. 1. This arrangement effectively produces a waveplate of variable thickness l' . If the axes of the waveplate have the same orientation as those of the wedge-pair then $l' = \Delta L + L_p$, where L_p is the thickness of the waveplate and ΔL is the thickness of the wedge-pair, which can be varied between ΔL_{max} and ΔL_{min} by changing the insertion of the wedges. However, if the waveplate is orientated with its axes at 90° to the axes of the wedge-pair then $l' = |\Delta L - L_p|$ since the phase-shift introduced in the waveplate will now be offset by that introduced in the wedge-pair. By choosing L_p such that $L_p = \Delta L_{min}$ it is possible to tune l' continuously from 0 to a maximum $\Delta L_{max} + L_p$ simply by varying the insertion of the wedge-pair and selecting the appropriate waveplate orientation.

In order to demonstrate this technique, cross-correlations of the pulsetrains were recorded for different wedge thicknesses and waveplate orientations. The pulse trains were formed by stretching 35fs pulses to approximately 10ps using a grating stretcher comprising a single 880 lines/mm Au-coated grating used at a 20° degree angle of incidence. The 1st order beam was reflected onto the grating four-times using the combination of a horizontal and vertical retro-reflector. The efficiency of the grating into 1st order was 80% so that the throughput of the stretcher was 40%. The stretched pulse was then passed through the wedge-pair-waveplate combination with its polarization at 45° to the axes of the variable waveplate. The wedge-pair used in these experiments comprised two quartz wedges, anti-reflection coated for 800nm, 25mm high and 50mm wide with thin and thick edges of 1mm and 15mm, respectively. The finite size of the laser beam limited ΔL_{min} to 8mm and ΔL_{max} to 24mm. The waveplate was a 7.7mm thick quartz plate, so that $L_p \approx \Delta L_{min}$. After the variable waveplate the stretched pulse

was passed through a linear polarizer, so that only the horizontal polarization was transmitted which, together with the stretcher efficiency, resulted in a total pulse train generation efficiency of 20%. We note that with an optimized stretcher design the efficiency of the pulse train optics could be increased close to the theoretical maximum efficiency of 50%.

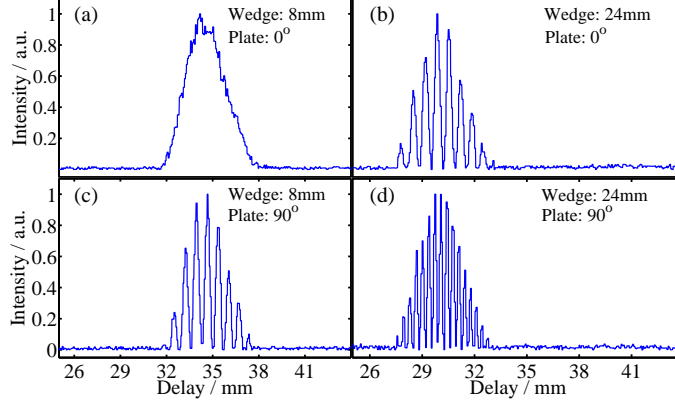


Fig. 2. Measured cross-correlations of pulse trains for: (a) $l' = |\Delta L_{min} - L_p|$, (b) $l' = |\Delta L_{max} - L_p|$, (c) $l' = \Delta L_{min} + L_p$, (d) $l' = \Delta L_{max} + L_p$.

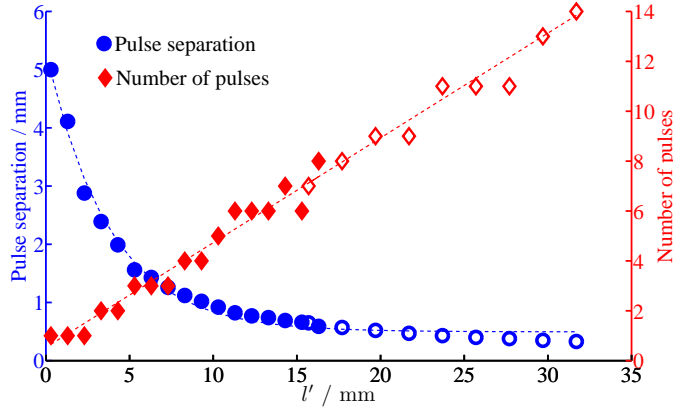


Fig. 3. Measured variation of pulse separation, d , and number of pulses, N , in the pulse train with effective waveplate thickness, l' . The open and closed symbols are for waveplate orientations of 0° and 90° , respectively. The dashed lines are fits to the measured data.

Fig. 2 shows the measured cross-correlations of the pulse trains generated using the extreme values of ΔL for both waveplate orientations, demonstrating that high contrast pulse trains are produced across the full range of l' . The robustness of this technique is illustrated in Fig. 2 (b) and (c), corresponding in both cases to $l' \approx 16$ mm. The resulting cross-correlations are shown to be almost identical, except for a temporal shift due to the optical path introduced by the difference in ΔL . The parameters of pulse trains generated by various values of l' and for different orientations of the wedge pair and waveplate are shown in Fig. 3. It is seen that $d \propto 1/l'$, as expected, and can be varied continuously from approximately 0.3 – 5mm. Since the total stretch of the pulse is determined by b , which is fixed by the grating stretcher, the number

of pulses $N \propto b/d \propto l'$, as confirmed by the data in Fig. 3.

3. Quasi-phase-matching with tunable pulse trains

3.1. Experimental setup

QPM using the pulse trains described above was studied using a 1 kHz Ti:sapphire laser system which produced linearly polarized pulses of energy of 2.8mJ, duration 35fs, and centre wavelength 800nm. A schematic diagram of the experimental arrangement is shown in Fig. 4. The output of the Ti:sapphire laser was split into a 0.6mJ driver beam used to generate harmonics and a 2.2mJ counter-propagating pulse used to generate the pulse train. The energy of each beam could be controlled independently by use of a waveplate-polarizer combination. The pulse train was generated by passing the counter-propagating pulse through the optical system described in the previous section. The point of collision between the driver and the pulse train could be varied using a computer-controlled timing slide. The polarization of the pulse train was parallel to that of the driver beam, with the result that the least amount of energy is required to achieve QPM [16].

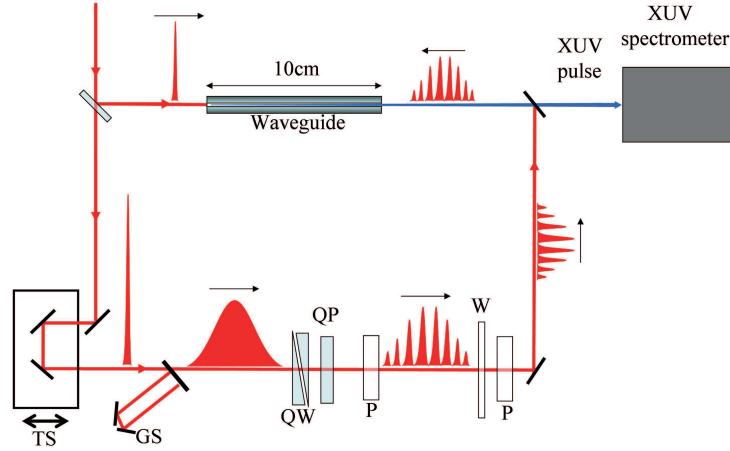


Fig. 4. Schematic of experimental setup. TS: timing slide, GS: grating stretcher, QW: quartz wedge-pair, QP: quartz plate, P: polarizer, W: $\lambda/2$ waveplate.

The driver beam and counter-propagating pulse train were coupled into opposite ends of a glass hollow-capillary waveguide using $f = 500\text{mm}$ lenses such that the focal spots of both beams were closely matched to the lowest-order mode of the waveguide. The waveguide was 100mm long with an inner-core diameter of $102\mu\text{m}$. Narrow slots were cut 2.5mm and 38mm from the exit (i.e the end closest to the spectrometer) of the capillary to allow gas to be injected into the waveguide. A similar slot was located 48mm from the exit, allowing gas to leave the waveguide. The short gas region and long run-in region of this waveguide design served to improve the mode quality of the driving laser pulse, while minimizing ionization-induced defocusing. The waveguide was filled with 14mbar of Ar gas through the slots at 2.5mm and 38mm, ensuring a constant pressure between these gas inlets. The transmissions of the driving beam and the pulse train were 55% and 50%, respectively. The generated harmonics passed through

a 2mm diameter hole in the mirror used to couple the counter-propagating beam into the capillary, and entered a flat-field spectrograph containing a gold-coated grating with a spacing of 1200 lines/mm and a cooled soft x-ray CCD.

3.2. Results

For various values of l' the harmonic spectrum was recorded (using 1s exposures) as a function of the collision point, z , of the driver and pulse train. As l' was increased from an initial value of 2mm suppression and coherent oscillations were observed for $q = 21 - 25$. As l' was increased further the harmonic showing the greatest QPM enhancement was shifted to higher orders, as d became matched to L_c . This behaviour is clearly seen in Fig. 5 which shows the normalized intensity in a 1nm bandwidth centred on each harmonic as a function of z for harmonics $q = 27 - 31$ at each value of l' . For increasing q the observed oscillations and enhancements are seen to occur at higher values of l' , corresponding to matching smaller values of L_c , as expected. It is also observed that for increasing q and l' the maximum enhancement which is achieved increases, since $N \propto l'$, enabling matching to occur over a larger number of zones at higher photon energies. We note that for the experimental arrangement described here true phase-matching by balancing the waveguide and plasma dispersion could only be achieved up to $q = 25$, however by varying l' it was possible to achieve QPM up to the cut-off harmonic, $q = 33$. In Fig. 5 the peak of the enhancements for each harmonic order is seen to shift to lower values of delay as l' increases due to the change in optical path as ΔL increases. Achieving the maximum enhancement via PTQPM for a particular harmonic order therefore requires both matching d to L_c , as well as optimizing the collision point within the waveguide.

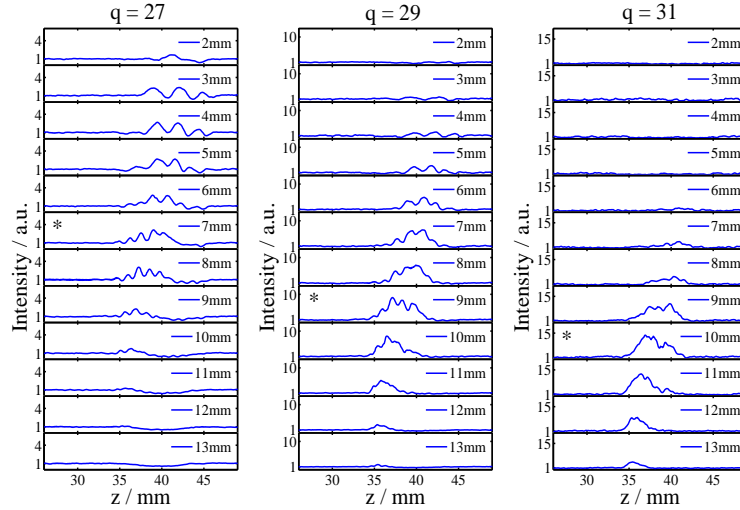


Fig. 5. Normalized harmonic signal in a 1nm bandwidth for harmonics $q = 27 - 31$ as a function of collision point for different values of l' . As q increases enhancements are observed to occur at larger values of l' , corresponding to matching shorter coherence lengths. The asterisk in each case indicates the value of l' at which the maximum enhancement is observed. The signal has been normalized to the average obtained in the same spectral window over 30 exposures in the absence of the pulse train.

Fig. 6 shows the spectrum of the generated harmonics in the absence of a pulse train. Also shown is the maximum signal which could be achieved for each harmonic order by PTQPM for optimized values of l' and the collision point. It can be seen that the output of each harmonic

can be optimized by correct tuning of the pulse train. Suppression, rather than enhancement, was observed for harmonics below $q = 25$, consistent with the fact that for these harmonics strong absorption and long coherence lengths prevent efficient QPM.

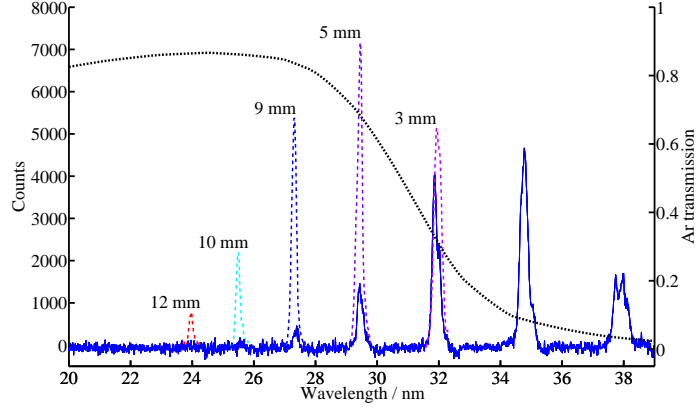


Fig. 6. Harmonic spectrum generated in 14mbar Ar in the absence of a pulse train (solid blue line). The dashed lines show the largest measured signal when the pulse train was present and l' and the collision point were optimized for that harmonic. The dotted black line shows the transmission through 5mm of 14mbar Ar (corresponding to the total length of the pulse train).

PTQPM requires sufficient intensity in the counter-propagating pulses to suppress HHG in regions of destructive interference. To understand this in detail the dependence of QPM on the intensity of the pulse train was therefore investigated for two pulse train configurations: $l' = 12\text{mm}$ corresponding to enhancement of $q = 31$, and $l' = 2\text{mm}$ corresponding to strong suppression of $q = 23$. For each configuration, scans were performed for different pulse train intensities. The results of these measurements are shown in Fig. 7. It can be seen that maximum suppression and enhancement for both low and high order harmonics occur at approximately 80% of the maximum counter-propagating beam intensity, demonstrating that the enhancements observed in these experiments are not limited by the intensity available in the counter-propagating pulse train.

The technique for generating pulse trains used in this experiment results in pulse trains of the form $A(z)\cos^2(2\pi z/d)$, as observed in the frame of the driving pulse, where $A(z)$ is the envelope of the pulse train. Each pulse in the train will therefore have a different peak intensity, and consequently will have a different contribution to QPM, depending on its position relative to the peak of the envelope. In addition, the shape of individual pulses within the train means that not all points on a pulse will result in the same level of suppression — points at the beginning of the pulse will have little effect, while those at the peak of the pulse will have the largest effect. Using the results of Fig. 7 it is possible to incorporate these effects into a simple numerical model of PTQPM. The expected output of harmonic q may be calculated by integrating the growth equation given by

$$\frac{dE_q}{dz} = s_q(z)\exp(-i\pi z/L_c) - \frac{\alpha_q}{2}E_q \quad (2)$$

where E_q is the amplitude, α_q is the power absorption coefficient of harmonic q [17], and $s_q(z)$ is the strength with which harmonics are generated. For these calculations the pulse train was

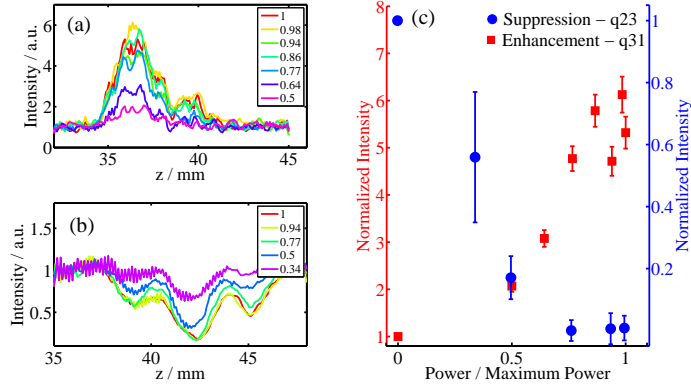


Fig. 7. (a) Normalized harmonic signal as a function of the collision point for different powers P of the pulse train for: (a) $q = 31$, $l' = 12$ mm; (b) $q = 23$, $l' = 2$ mm. (c) Measured suppression of $q = 23$ (blue circles) and enhancement of $q = 31$ (red squares) as a function of P . The pulse train power has been normalized to the maximum pulse train power.

modeled as $p(z) = \exp(-z^2/2\sigma^2)\cos^2(2\pi z/d)$, where 2σ is the $1/e^2$ half-width of the pulse train measured in the laboratory frame. The intensity dependence of the harmonic suppression was modelled by assuming $s_q(z) = 1 - F(p(z))$, where F is a threshold function such that $F = 1$ for $p(z) > 0.8 = 1$ and $F = 0$ for $p(z) < 0.3 = 0$, as observed experimentally. The enhancement in this model was determined by integrating Eqn. 2 over a fixed number of coherence lengths with the pulse train modulation, and then normalizing this with the integrated output without the pulse train modulation ($s_q(z) = 1$ at all points). For each harmonic order, L_c was determined from the matching condition ($d = 2L_c$), using the fit to the measured values of d shown in Fig. 3.

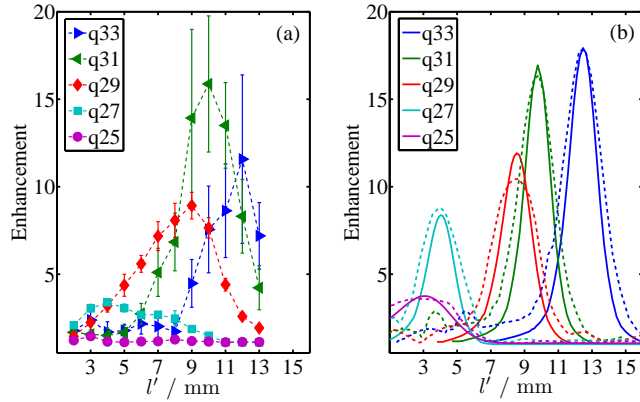


Fig. 8. (a) Maximum measured enhancement of harmonic orders $q = 25 - 33$ as a function of l' . (b) Calculated enhancement of harmonic orders $q = 25 - 33$ as a function of l' (dashed lines) including the intensity dependence of the harmonic suppression as measured experimentally. The solid lines in (b) show the calculated enhancements of harmonic orders $q = 25 - 33$ without including the intensity dependence of the harmonic suppression.

The maximum measured enhancements for harmonic orders $q = 25 - 33$ at each value of

l' , as well as the calculated enhancements, are shown in Fig. 8. Broad qualitative agreement is seen between the experimental results and calculated enhancements. The maximum measured enhancement shifts to higher values of q as l' is increased, as expected. Enhancements can be tuned up to the cutoff harmonic, with a 16-fold increase in signal being observed for $q = 31$, corresponding to an estimated mean photon flux of 7×10^7 photons sec^{-1} . This estimation is based on the transmission of the aluminium filters in the spectrograph, the grating efficiency, and the quantum efficiency of the CCD camera at this photon energy. It is also observed that as l' increases so too does the enhancement, since $N \propto l'$ allowing PTQPM to be achieved over a larger number of zones. The calculated harmonic enhancements in Fig. 8 (b) show that the intensity dependence of the harmonic suppression only results in a slight increase in the range of values of l' for which QPM is observed and does not have a large impact on the resulting enhancements. The lower than expected enhancements observed for $q = 25$ and 27 compared with the calculated enhancements of these harmonics may be due to longitudinal variation of L_c , preventing the output of multiple in-phase zones to coherently combine. It has previously been shown that even small changes in L_c are sufficient to prevent PTQPM over multiple zones [11]. The measured and calculated enhancements also show that the range of l' for which significant enhancement is observed becomes narrower for increasing q . This narrowing occurs because QPM becomes increasingly selective of a particular harmonic order as the number of contributing zones increases due to the increasing number of pulses in the train, as has previously been demonstrated in the case of PTQPM [10].

4. Conclusion

We have demonstrated a method for generating continuously tunable pulse trains and shown that they can be used for quasi-phase-matching high-order harmonics. Tuning of the QPM spectrum was demonstrated over a range of harmonic orders up to the harmonic cut-off by tuning the pulse train parameters. A maximum QPM enhancement of more than an order of magnitude was observed for $q = 31$, and a simple numerical model was found to be in good agreement with the data. The pulse trains generated in this work are scalable to large numbers of pulses, can match to coherence lengths on the order of tens of microns, and in principle may also be used to generate pulse trains with nonuniform d [18]. The ability to match to short coherence lengths combined with the favourable scaling of increasing N for decreasing values of d afforded by these pulse trains offers an attractive route for achieving high-brightness tunable QPM sources at photon energies well beyond those which are possible with true phase-matching.

5. Acknowledgements

This work was supported by the Engineering and Physical Sciences Research Council under grant EP/G067694/1.